Localization and socialization: Experimental insights into the functional architecture of IP_3 receptors

Luis Diambra[1] and Jonathan S. Marchant[2,a)]
[1]*Laboratorio de Biología de Sistemas, CREG-UNLP, Av Calchaqui 23500, CP 1888, Buenos Aires, Argentina*
[2]*Department of Pharmacology, University of Minnesota Medical School, Minneapolis, Minnesota 55455, USA*

(Received 18 February 2009; accepted 11 May 2009; published online 18 September 2009)

Inositol 1,4,5-trisphosphate (IP_3)-evoked Ca^{2+} signals display great spatiotemporal malleability. This malleability depends on diversity in both the cellular organization and *in situ* functionality of IP_3 receptors (IP_3Rs) that regulate Ca^{2+} release from the endoplasmic reticulum (ER). Recent experimental data imply that these considerations are not independent, such that—as with other ion channels—the local organization of IP_3Rs impacts their functionality, and reciprocally IP_3R activity impacts their organization within native ER membranes. Here, we (i) review experimental data that lead to our understanding of the "functional architecture" of IP_3Rs within the ER, (ii) propose an updated terminology to span the organizational hierarchy of IP_3Rs observed in intact cells, and (iii) speculate on the physiological significance of IP_3R socialization in Ca^{2+} dynamics, and consequently the emerging need for modeling studies to move beyond gridded, planar, and static simulations of IP_3R clustering even over short experimental timescales. © *2009 American Institute of Physics*. [DOI: 10.1063/1.3147425]

Changes in cytoplasmic Ca^{2+} concentration control the activity of numerous cellular proteins. Inositol 1,4,5 trisphosphate receptors (IP_3Rs) localized on the endoplasmic reticulum play a key role in regulating cellular Ca^{2+} homeostasis by controlling Ca^{2+} flux into the cytoplasm from this intracellular Ca^{2+} store. IP_3R stimulation results in complex spatial and temporal patterns of intracellular Ca^{2+} release activity. Consequently, the utility of computational approaches in recapitulating and predicting Ca^{2+} release dynamics requires accurate definition of the subcellular dynamics and *in situ* functionality of cellular IP_3Rs. This review summarizes experimental data underpinning our current understanding of the functional architecture of IP_3Rs in the endoplasmic reticulum, to highlight the need for the next generation of modeling studies to consider the functional ramifications of IP_3R socialization within diverse and dynamic architectures in live cells.

I. INTRODUCTION

The cellular architecture of IP_3Rs is diverse: Their global distribution is not uniform, and their localized organization is not stereotypic. This organizational diversity is significant for patterning Ca^{2+} transients, crudely by dictating the targeting and propagation of Ca^{2+} signals ("localization"), but likely also by impacting the functional properties of IP_3Rs within the native membranes where they reside ("socialization"). Therefore, from an experimentalist's perspective, predictive modelling of cellular Ca^{2+} signals necessitates dissecting the "functional architecture" of IP_3Rs,[1] to reflect both the cellular organization and unitary *in situ* properties of these channels, as well as the dynamic interdependence of these two considerations. This brief review will summarize recent experimental data on this theme, addressing the cellular organization of IP_3Rs from the macroscopic (cellular, "global") down to the microscopic (subcellular, "local") scale, ensuing ramifications for IP_3R function, and emerging modeling attempts to predict the dynamics and properties of IP_3Rs in different states of organization within realistic cellular geometries.

II. THE GLOBAL DISTRIBUTION AND LOCAL ORGANIZATION OF IP_3RS IS INHOMOGENOUS

There can be considerable macroscopic heterogeneity in IP_3R localization throughout the cell, both within and beyond the bulk endoplasmic reticulum (ER) (see Ref. 2 for a review). This is best exemplified in the gradients of IP_3R localization in polarized cells demonstrated by antibody/fluorescent ligand labeling, fractionation, and functional Ca^{2+} imaging approaches, as well by resolution in electron micrographs of variable IP_3R densities between different subcellular regions of ER.[3–9] Similarly, targeting of IP_3R outside the "bulk" endoplasmic reticulum—at the cell surface,[10] in other organelles,[11,12] or within deep nuclear projections[13]—may further bias IP_3R distribution across the cell. Such gradients in endogenous IP_3R localization are crucial for cellular physiology by impacting resting Ca^{2+} gradients, as well as the initiation and the spatiotemporal dynamics of agonist-evoked Ca^{2+} signals. Often these differential distributions derive from differential targeting of IP_3R isoforms,[2,6,7,14,15] but regionalization also occurs in cells where a single IP_3R iso-

a)Author to whom correspondence should be addressed. Electronic mail: march029@umn.edu. Telephone: 612-624-6687.

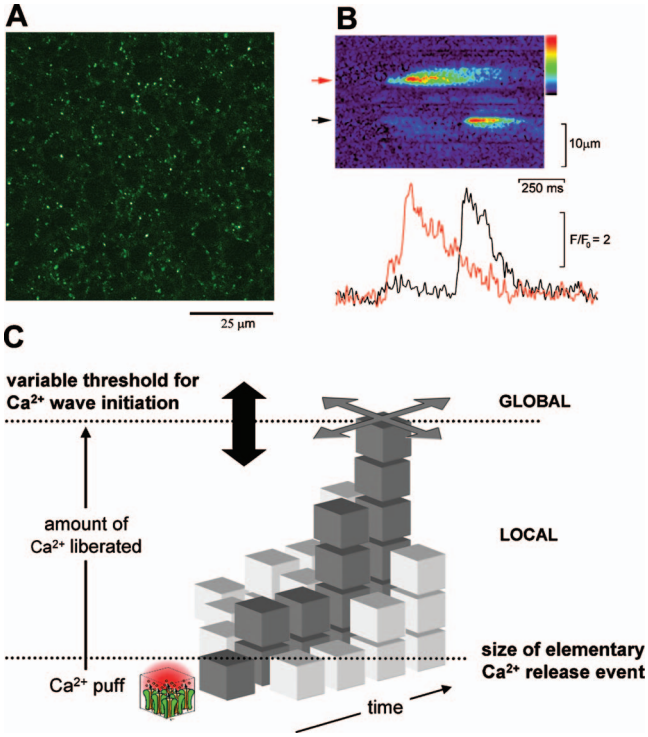

FIG. 1. (Color) Structural, functional, and conceptual views of native IP_3R architecture in the *Xenopus* oocyte. (a) Punctate immunolocalization of native clusters of IP_3Rs in the cortical ER of a *Xenopus* oocyte resolved by immunofluorescence. (b) Top: linescan image of two discrete Ca^{2+} puffs resolved using fluo-4 (K_d for Ca^{2+}= ~345 nM) that were evoked by photorelease of IP_3. Bottom: associated fluorescence profiles. (c) Schematic model, combining (a) and (b), conceptualizing Ca^{2+} puffs as the local elementary Ca^{2+} release occurring from discrete IP_3R clusters (cubes) spaced throughout the ER. Summation of the stochastic behavior of these elementary events is required to trigger a Ca^{2+} wave and establish repetitive Ca^{2+} oscillations. Ca^{2+} puffs occur independently at low levels of stimulation, but activity is coordinated by Ca^{2+} during maintained stimulation (*x*-axis) to trigger a global whole-cell Ca^{2+} signal. This summation is often coordinated by the activity of particular "focal" Ca^{2+} puffs sites (dark gray) that serve as the spatial focus of wave initiation. In the *Xenopus* oocyte, the amount of Ca^{2+} liberated by a Ca^{2+} puff is well below the threshold to initiate a Ca^{2+} wave, allowing the coexistence of local and global signaling modalities in the same cell.

form predominates (for example, Refs. 1, 9, and 16–18). Indeed, there is growing molecular insight into mechanisms dictating IP_3R localization in diverse cell types.[2,19,20] While, obviously, graded spatial expression is but one way to variegate intracellular Ca^{2+} release activity, it provides a simple route to customize cellular Ca^{2+} signals.

Similarly, at the microscopic level, the local organization of IP_3Rs within the ER is not homogenous. First, in peripheral ER closely juxtaposed to the cell surface, IP_3Rs frequently show punctate distributions within signaling complexes, localized by molecular interactions unique at this interface. The existence of such IP_3R-enriched "microdomains" identified in diverse cell types, serve to define agonist specificity and/or initiation sites of Ca^{2+} signals.[21–28] Within nonperipheral ER, both structural and functional data suggest that IP_3Rs are gregarious, organizing into discrete "clusters" in "unstimulated" cells. For example, antibody staining reveals punctuate IP_3R immunoreactivity throughout the ER in primary [Fig. 1(a)] (Refs. 16 and 29–31) and immortalized cells,[32,33] a conclusion also supported from a more limited pool of electron microscopy-based analyses.[9] While careful collection and processing of immunocytochemical datasets can provide quantitative insight into the number, three dimensional distribution and properties of endogenous Ca^{2+} channel clusters,[34,35] such methods have not yet been applied to IP_3Rs. Consequently, the majority of evidence supporting a native, clustered organization of IP_3Rs derives from functional rather than structural measurements, specifically electrophysiological analyses of endogenous IP_3R distributions in excised nuclei[36,37] and predominantly from confocal Ca^{2+} imaging in intact cells.[38,39]

Rapid, confocal Ca^{2+} imaging methods revealed that IP_3-evoked Ca^{2+} release from the ER was a discontinuous process, by demonstrating discrete and recurrent sites of Ca^{2+} release spaced throughout the ER. At low levels of stimulation, localized Ca^{2+} release events occurred at these sites spreading for a only few micrometers and persisting for a few hundred milliseconds [Fig. 1(b)]. These rapid, transient Ca^{2+} release events were christened Ca^{2+} "puffs"[40] and combined experimental and modeling analyses of Ca^{2+} puff properties have established that they result from the coordinated opening of a small number of Ca^{2+} channels.[41,42] Similar "elementary" responses mediated by clusters of ryanodine receptors, the other major class of intracellular Ca^{2+} channels are discussed elsewhere.[43,44] The variabilities in the amplitude of successive Ca^{2+} puff events and peak amplitude of Ca^{2+} puffs resolved at the same site suggest that not all IP_3Rs open during a Ca^{2+} puff and that the underlying number of clustered receptors varies between Ca^{2+} release sites.[41,42] A recent experimental estimate, calibrating probable single channel responses ("Ca^{2+} blips") to subsequent Ca^{2+} puffs that they rapidly trigger suggest between ~6 and 60 IP_3Rs open during a Ca^{2+} puff.[45] Deterministic simulations of the fluorescence profiles of these coupled events further refine these experimental estimates to suggest that Ca^{2+} puffs could result from the activity of ~25–35 IP_3Rs that simultaneously open for ~20 ms.[46] While such values derive from well considered calculations, it should be remembered that the variability in these estimates is trivial compared to the effects of a small variation in key parameters used to derive these estimates.

The observations that (i) Ca^{2+} puffs are rapidly evoked by photorelease of IP_3, with observed latencies [>250 ms[47]], attributable to a local requirement for Ca^{2+} activation,[48] (ii) isolated Ca^{2+} blips are rare events,[41] (iii) Ca^{2+} wavefronts are saltatory,[47,49] reflecting progressive activation of proximal IP_3R clusters, and (iv) that the kinetic profiles Ca^{2+} puffs are similar in many diverse cell types expressing different IP_3R isoforms[50] support the concept that the basal architectural state for IP_3R organization comprises small clusters of IP_3Rs spaced throughout the ER. To the best of our knowledge, Ca^{2+} puff-like signals have not been resolved in invertebrate systems (but see Ref. 37), reflecting a general lack of insight into the molecular basis of IP_3R clustering behavior and the timing of its evolutionary emergence.

Therefore, Ca^{2+} puffs represent the basic building blocks from which whole cell Ca^{2+} signals are assembled. At higher levels of IP_3, Ca^{2+} puff frequency is increased and their

proximal activity coordinated by Ca^{2+} to repeatedly trigger Ca^{2+} waves that spread between neighboring Ca^{2+} release sites before inhibitory cues restrain Ca^{2+} release activity.[48,51,52] Often, this behavior is entrained by the higher activity of unique Ca^{2+} puff sites that serve as the focus for Ca^{2+} wave initiation,[52–54] demonstrating that IP_3Rs clusters in proximal ER regions can display different activities. The mechanistic basis for the higher IP_3R sensitivity at these sites remains unclear. Physiological cues control the positioning of the regenerative threshold relative to the size of the fundamental Ca^{2+} release event [Fig. 1(c)], thereby coordinating the predominance of local or global Ca^{2+} signaling domains with cellular physiology.[1,55] In summary, this model derived from Ca^{2+} imaging data has had significant value in conceptualizing how Ca^{2+} waves trigger and propagate via summation of localized activity of clustered IP_3Rs.

A key caveat is that this interpretation entirely derives from functional measurements of open channels, reported via changes in the fluorescence of high affinity Ca^{2+} indicators with limited kinetic resolution. Therefore, while considerable effort has been spent, for example, (re)estimating the number of active channels during a Ca^{2+} puff, comparatively little is known about the underlying structural architecture of IP_3Rs beyond what has been inferred from divination of Ca^{2+} release profiles collected at high temporal resolution. Outstanding issues are insight into (i) the *total* number of IP_3Rs within a native cluster[56] (what is the open probability of an IP_3R during a Ca^{2+} puff?), (ii) cluster microarchitecture (how are IP_3R packed within a Ca^{2+} puff site?) and (iii) clustering mechanisms [what is the molecular basis of cluster (dis)assembly *in vivo*, the stoichiometry of accessory proteins if required, and by extension the mechanism that delimits native cluster size?]. These structural issues are interrelated, for example, observation of propagating "microwaves" within single Ca^{2+} puff sites[49,57] and the observation of Ca^{2+} blip-like "triggers" preceding Ca^{2+} puffs[45] implies a small number of loosely corralled IP_3Rs [mean separation several fold greater than the lateral dimensions of a tetrameric IP_3R (Refs. 46, 58, and 59)] with relatively high open probability. Alternatively, clusters may consist of a higher number of more tightly packed channels (exemplified by the lateral arrays of IP_3Rs resolved in cerebellum[60]) but with much lower likelihood of individual activation. IP_3R density also imposes spatial constraints on potential molecular mechanisms for cluster formation and functional recruitment, whether bridging via accessory proteins or direct interactions between adjacent IP_3R tetramers will suffice, and whether activation/inactivation is supported solely by Ca^{2+} feedback or by conformational spread between physically coupled Ca^{2+} adjacent channels.[61–65] Finally, and possibly most importantly in terms of cellular physiology, there has been until recently[66] little experimental insight into the functional consequences of socialization into clusters on the unitary properties of the IP_3Rs (see Sec. IV and the review by Taylor's group in this issue), let alone simultaneous structural/functional analyses of different IP_3R architectures within the same cell.

III. THE ORGANIZATION OF ER, AND IP_3RS WITHIN IT, IS MALLEABLE AND INDEPENDENT

Compartmentalization of Ca^{2+} signals results not only from static heterogeneities in the distribution of Ca^{2+}-handling proteins but also from dynamic changes in the positioning of the ER, and via reorganization of IP_3Rs independently from changes in ER morphology. There is a growing awareness of the importance of these changes in patterning Ca^{2+} signals over physiologically relevant timescales, and consequently the need for realistic representation of this architecture in predictive models of Ca^{2+} dynamics.

ER dynamics. The ER is a highly dynamic organelle that adapts in organization both in response to cellular activity and preparatively for transitions in cellular physiology. Pathological cues also impact ER morphology, and consequently IP_3R localization.[67,68] Morphological alterations of the ER can be dramatic (major repositioning,[69] reorganization,[1,3,59,70,71] or more subtle alterations in the prevalence of subdomains that are constantly remodelling.[72,73] Physiological[72] (and protracted[74]) changes in cytoplasmic Ca^{2+} concentration ($[Ca^{2+}]_{cyt}$) regulate ER architecture by regulating a growing list of Ca^{2+}-dependent effectors controlling ER structure,[75,76] and reciprocally a changing ER architecture will impact cellular Ca^{2+} dynamics by redistributing ER-associated Ca^{2+} channels, pumps, and effectors throughout the cell.

IP_3R dynamics. While macroscopic reorganizations of the ER indirectly move IP_3Rs around the cell, changes in steady-state IP_3R localization[14,31,77] and organization[32] can occur independently of major alterations in ER structure, as also seen with other components of the cellular Ca^{2+} homeostatic machinery.[78,79] Live cell imaging studies of fluorescent-protein tagged IP_3Rs have provided quantitative insight into the dynamics of IP_3Rs within the ER in live cells.[80–82] Although it is appreciated that overexpressed IP_3Rs may not faithfully report native IP_3R behavior,[80,83] it appears that the majority of cellular IP_3Rs are mobile and free to diffuse throughout the ER. Diffusibility (~100-fold range in estimates, Table I) is regulated by accessory proteins selective for specific IP_3R isoforms,[81] and by interaction with other IP_3Rs.[33] Of particular relevance to the topic of this review is the observation originally made by Wilson *et al.*[32] that endogenous IP_3Rs transiently aggregate during protracted stimulation into "larger IP_3R clusters" [average diameter, 0.35–2.3 μm (Ref. 84)] that then dissociate following agonist removal. Estimates of IP_3R diffusibility (Table I) are compatible with the observed density of IP_3R clusters: For example, in RBL-2H3 cells,[33] an IP_3R would diffuse through a surface area of ~30 μm^2 over a 10 min period, a territory likely containing several IP_3R aggregates (~1 per 10 μm^2). This clustering behavior has been reported in several cell lines (Table II), and crucially is recapitulated when IP_3R constructs are overexpressed, thereby providing mechanistic insight into this phenomenon in live cells. Such studies[33,84–86] have shown the following.

(i) All IP_3R isoforms display activity-induced reorganization,[84] but cluster dimensions are shaped by

TABLE I. IP_3R mobility within the ER. Examples of FRAP-derived estimates for the diffusion coefficient and mobile fraction of fluorescent-protein tagged IP_3Rs in different cell types. Please refer to references for details of how these parameters were calculated in individual studies (n.r.=not reported).

Cell type	IP_3R isoform	Diffusion coefficient ($\mu m^2/s$)	Mobile fraction	Reference
MDCK (10B)	IP_3R1-GFP	0.004–0.01	100%, decreasing to 64% in bulk ER after polarization	82
CHO-K1	GFP-IP_3R3	0.031	67%	80
COS-7	GFP-IP_3R3	0.044	77%	80
RBL-2H3	YFP-IP_3R1	0.056	76%, decreasing to ~69% after IP_3R clustering	33
Hippocampal neurons	GFP-IP_3R1	0.26	n.r.	81
	GFP-IP_3R3	0.45		

the presence of specific IP_3R isoforms (but see Ref. 33).

(ii) Cluster formation does not parallel major ER structural changes.[33,85,86] Indeed, one report demonstrates IP_3Rs aggregate even within vesicularized ER (Ref. 85) (contrast with Ref. 86). Once formed, clusters are motile within contiguous ER and expand in size either via fusing with other clusters[86] or growing by further IP_3R entrapment.[33,86]

(iii) Protracted exposure to high concentrations of agonist, or IP_3,[85] is needed to induce IP_3R aggregation (Table II). Kinetically, this behavior occurs over a time frame of minutes, delayed [lags of ~60–90 s (Refs. 85 and 86)] to the initial agonist-evoked Ca^{2+} signal(s). Cluster disassembly occurs over a similar time frame, during[85] or following agonist removal,[86] likely by progressive attrition of clustered IP_3R. While this phenomenon has been extensively examined in two specific cell lines (Table II), it is less apparent in other cells without further manipulation of stored/extracellular Ca^{2+}.[85] Given the intensity of cellular stimulation required to trigger this behavior, the relationship of this mechanism to physiological "clustering" paradigms[87] and agonist-evoked Ca^{2+} spiking is unclear. For example, IP_3R1 and IP_3R3 are proposed to play opposing roles in facilitating and inhibiting Ca^{2+} oscillations,[88] but both form similar aggregates during stimulation.[84]

(iv) IP_3-evoked conformational change(s) is crucial in inducing higher-order IP_3R clustering. Binding-deficient mutants of individual IP_3R isoforms, as well as a natural binding-deficient IP_3R2 splice variant, fail to aggregate on cellular stimulation even as heteromultimers.[84,86] More crucially, mutants competent at IP_3 binding but defective in the ensuing conformational movements that lead to channel activation fail to cluster. These mutational analyses represent a compelling argument that an IP_3-evoked conformational change—independent of any Ca^{2+} flux through the channel[86]—controls IP_3R aggregation. Resolution of pre-existing clusters in unstimulated cells that endogenously[32,33] or heterologously express IP_3R2

TABLE II. Activity-induced clustering of IP_3Rs in various cell lines. Summary of studies investigating the formation and properties of IP_3R clusters evoked by cellular stimulation. Readers are referred to indicated references for further experimental detail. Exogenous IP_3R constructs were expressed by transient transfection, unless indicated otherwise.

Cell type	IP_3R isoforms	Stimulus (cell surface)	Kinetic insight	Reference
RBL-2H3	Endogenous IP_3R2	Antigen, postpriming	Greater than three fold increase in number of IP_3R cluster within 10 min	32
RBL-2H3	Endogenous IP_3R2	Antigen	Clusters apparent after 30 min in periphery of permeabilized cells	108
RBL-2H3	Endogenous IP_3R2; Expressed YEP-IP_3R1	Antigen, postpriming	Increase in cluster size, not number (at least for endogenous IP_3R2) maximal by 10 min	33
COS-7	Expressed GFP-IP_3R1	ATP (10 μM)	Onset of ~1 min, progressive increase in number during agonist exposure, delayed relative to $[Ca^{2+}]_{cyt}$ changes	86
COS-7	Expressed IP_3R1, IP_3R2 (SI_{m2+}, SI_{m2-}), IP_3R3	ATP (1 mM)	Analyzed after 20 min of ATP exposure. IP_3R2 (SI_{m2+}) clustered in unstimulated cells	84
COS-7	Expressed GFP-IP_3R3	ATP (100 μM)	Average onset of ~1 min, reversal within 20 min despite continued stimulation	85
HSY-EA1	Expressed GFP-IP_3R3 (stable cell line)	ATP (100 μM)	Clustering observed only in 10% of intact cells treated with ATP.	85
$E36^{M3R}$	Endogenous IP_3R2	Carbachol (1 mM)	Maximal after 30 min, reversed 30 min after agonist removal	
AR4-2J	Endogenous IP_3R2	CCK (0.5 μM)	Maximal by 30 min	32

(Ref. 84) has been suggested to relate to the higher IP_3 binding affinity of IP_3R2 relative to other IP_3R isoforms, such that ambient IP_3 levels are sufficient to adoption of a widespread, clustered architecture.[84]

Understanding such a conformer-dependent reorganization necessitates definition of the relevant IP_3-induced conformational change within tetrameric IP_3Rs that promotes aggregation. Single particle analysis of IP_3Rs has revealed significant ligand-induced changes in IP_3R structure (albeit Ca^{2+}-evoked changes[89]) that would likely impact cluster microarchitecture depending on the state of channel activation. For example, the transition between "compact" and "windmill" IP_3R structures[89] is striking (~1.5-fold change in diameter/cross sectional surface area), and may be of sufficient magnitude to impose conformational restrictions on activation, if packing density is too high, or inactivation and resensitization if active conformers sterically trap neighbors in conformations ("conformational locking") that persist beyond ligand dissociation from individual channels. Consequently, the interrelationship between agonist occupancy, efficacy at promoting conformational changes and the ensuing initiation and reversal of clustering requires further experimental and modeling insight.

IV. IP_3RS ARE GREGARIOUS, BUT THE FUNCTIONAL RAMIFICATIONS OF SOCIALIZATION APPEAR BIPHASIC

From the preceding discussion, it is clear that cellular IP_3Rs are gregarious and dynamically reorganize between heterogeneous populations of "clustered" architectures. Is IP_3Rs functionality regulated by this reorganization? Experimental studies with other membrane proteins have demonstrated that clustering regulates signaling activity, and reciprocally, signaling activity impacts clustering.[90–96] This reciprocity ensures diversity in cellular receptor architectures such that—as with IP_3Rs—native clusters of receptors, often too small to be resolved by confocal microscopy, are distinct from activity-induced aggregates. Functionally, the effects of receptor clustering can be manifest as either social excitability or inhibition, achieved through modulation of ligand sensitivity, channel transition rates, dynamic range, and the spatial spread of information at a cellular level.[90,97–100] Proposed mechanisms underpinning differential receptor behavior in clusters expand beyond effects of scaling in terms of increased receptor number and encompass the potential for amplification via activity-spread throughout the cluster, changes in the probability or kinetics of ligand (re)binding/dissociation consequent to clustering, or alerted ligand avidity owing to the adoption of a distinct receptor conformation or microarchitecture as a prerequisite for cluster formation. For IP_3Rs, feedback regulation by Ca^{2+} provides an additional level of interchannel regulation that, on the basis of quantitative modeling studies, has been shown to vary for different cluster microarchitectures,[64,65,101] and more generally as a consequence of clustering itself[66] (see also review by Taylor's group, this issue).

Therefore, in terms of terminology, it is clear that cluster has been used as a qualitative catch-all in the IP_3R literature to describe a broad scale of native and activity-induced IP_3R architectures. Although this descriptive sleight covers our lack of knowledge of microscopic IP_3R organization, it is problematic as it likely collates distinct basal and adaptive IP_3R architectures with divergent functional properties. Although this issue has not been directly addressed experimentally (e.g., by simultaneously imaging the structure and functionality of tagged IP_3Rs), several pieces of data suggest that large scale aggregation attenuates IP_3R activity. First, the stimulation paradigms that induce IP_3R aggregation require protracted exposure to high agonist concentrations (Table II) and consequently aggregation lags initial agonist-evoked Ca^{2+} signals.[33,85,86] This likely correlates with depleted ER Ca^{2+} stores (addition of Ca^{2+} to permeabilized cells prevents IP_3R aggregation[85]), a condition known to decrease IP_3R sensitivity.[102] Notably, the duration of photolysis-evoked Ca^{2+} transients is reduced following formation of IP_3R aggregates in RBL cells.[101] Second, ERp44 targets to IP_3R1 aggregates.[86] This ER lumenal protein inhibits the activity of the ubiquitously expressed IP_3R1.[103,104] Third, most generally, other scenarios of increased IP_3R density are associated with decreased IP_3R sensitivity. Specialized regions of the ER in oocytes with high IP_3R density[1,59] show attenuated local Ca^{2+} release activity until these domains are physiologically remodeled during oocyte maturation. In cerebellar Purkinje cells, electron microscopy-level resolution of ER regions with high IP_3R density[9,60,105] (approximately ten times density of adjacent ER,[9] or as physically coupled IP_3R arrays[60]) that increase during hypoxia is speculated to be an adaptation to decrease ER Ca^{2+} efflux. Collectively, such data suggest high density packing of IP_3Rs or activity-induced aggregation suppresses IP_3R activity.[1,85,101] Stochastic and deterministic modeling analyses also support this contention, justifying a conceptual separation of native, IP_3R clusters, optimized for generating the hierarchical diversity of Ca^{2+} signals,[106,107] from higher order IP_3R "aggregates" that attenuate Ca^{2+} release from the ER.[101] Although the functionality at the extremes (clusters versus aggregates) is different, the formation of these structures may nevertheless be underpinned by a conserved mechanism (IP_3-evoked IP_3R clustering) that spans the architectural continuum.

Therefore, the Ca^{2+} releasing ability of clusters may not equate with a proportional scaling of single channel activity (as assumed in many modeling analyses), rather IP_3R socialization may lead first to a disproportional facilitation of Ca^{2+} release activity in small IP_3R clusters that generate Ca^{2+} puffs, and then repression of IP_3R responsiveness in larger, activity-induced IP_3R aggregates (Fig. 2). Little is known quantitatively about transitions between these states and clearly further experimental and modeling insight is needed. At odds with this model is that suggestion that $IP_3R2(SI_{m2+})$ clusters, observed in resting COS-7 cells, represent native Ca^{2+} puff sites. Although their dimensions are smaller (greater than fourfold) than clusters formed by IP_3R1 or IP_3R3 in stimulated cells, this proposal appears premature in the absence of simultaneous structural/functional measurement. IP_3R1 and IP_3R3 do not form similar clusters in resting cells,[84] but Ca^{2+} puff kinetics are similar in cells enriched in these different IP_3R isoforms.[50]

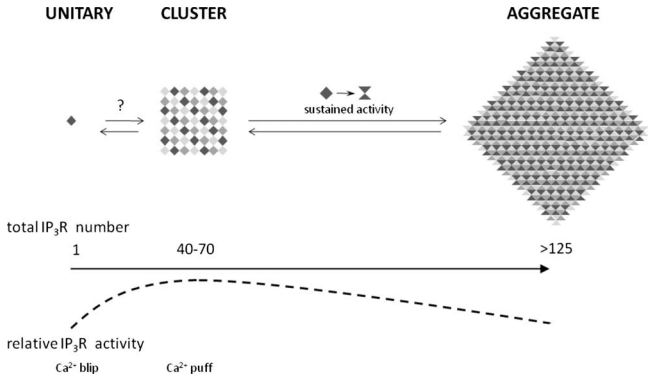

FIG. 2. Functional architecture of IP_3Rs—structural and functional distinction of native clusters and activity-induced aggregates. IP_3R socialization from (i) "unitary" channels to (ii) native clusters that support Ca^{2+} puffs to (iii) larger IP_3R aggregates observed following sustained stimulation. While little is known about mechanisms regulating cluster assembly, a change in IP_3R conformation (e.g., diamond to hourglass) is a prerequisite for aggregate formation. The functional effects of IP_3R socialization may not scale linearly with channel number, rather different architectures reflect distinct states of IP_3R activity: native "loose" clustering promotes IP_3R activity, whereas high density packing or activity-induced aggregation attenuates IP_3R activity. Numerical estimates are from Refs. 45, 56, and 101. For clarity, individual tetramers are represented in different shades of gray.

V. DYNAMIC IP_3R ARCHITECTURES, REALISTIC CELLULAR GEOMETRIES: RAMIFICATIONS FOR MODELLING

Experimental data have resolved a broad scope of cellular IP_3R architectures (from isolated channels to a heterogeneous population of higher-order structures exhibiting different organizations and functionalities). Appreciation of the diversity and dynamic malleability of IP_3R organization, and of the ER itself, poses a considerable challenge for *in silico* modelling. For reasons of obvious simplification, studies are frequently based on dimensionless representations of monotypic IP_3R clusters within gridded, static, planar arrays. Clearly, this neither represents *in vivo* IP_3R dynamics nor implicitly considers the effect of IP_3R organization on IP_3R behavior. Modelling an IP_3R cluster either as a collective of functionally independently channels or as an extrapolated multiple of the properties of an isolated IP_3R, while iterative, has been proven precariously assumptive especially in the absence of experimental insight into the ultrastructural basis of local Ca^{2+} signals. Although this broad architecture theme is not new (judiciously addressed over a decade ago in terms of ultrastructural limitations for channel synchronization by Ca^{2+}-induced Ca^{2+} release rather than conformational coupling[64]), its importance is being resuscitated by recent computational analyses.[35,46,65,101] Especially significant is the transition toward modelling Ca^{2+} channel architectures within realistic cellular geometries.[35,101] Notable, in the context of this review, are results such as those reported by Means *et al.*[101] that address the functional effects of transitions between different IP_3R architectures, including analyses within a realistic rendering of ER morphology. Stochastic and deterministic simulations comparing two states—diffuse versus aggregates observed on protracted stimulation (predicted to comprise of ~125 IP_3R2 channels)—suggest that aggregation reduces IP_3R open probability and the rate of Ca^{2+} release from the ER as a result of differential local Ca^{2+} feedback regulation. In this study, social inhibition of proximal IP_3Rs was predicted even in loosely coupled aggregates (more analogous to Ca^{2+} puff architecture) albeit only from deterministic openings of a small proportion ($<3\%$) of colocalized IP_3Rs. Clearly, more extensive simulations are required, but incorporation of biologically relevant architectures[35,101] is a major step forward toward predictive models of macroscopic Ca^{2+} dynamics. Future studies will likely incorporate IP_3R dynamics and the real-time (dis)assembly of different IP_3R clustered architectures, as well as physiological relevant changes in ER organization and Ca^{2+} homeostasis.

In summary, it is clear that cellular IP_3R architectures are dynamic and diverse. Comparatively little quantitative insight is available regarding the endogenous ultrastructural organization of IP_3Rs or the functional impact of these different IP_3R architectures in gearing IP_3R responsiveness. However, the ability of cells to remodel IP_3Rs into architectures with different functionalities likely provides flexibility in adapting to physiological cues and withstanding pathological insults. Appreciation of this functional architecture of IP_3Rs is therefore essential in developing models to faithfully capture the full range of ER Ca^{2+} release profiles in any given cell type.

ACKNOWLEDGMENTS

Work is supported by NIH (Contract No. GM088790) and NSF (J.S.M.) and CONICET-Argentina (L.D.).

[1] M. J. Boulware and J. S. Marchant, Curr. Biol. **15**, 765 (2005).
[2] E. Vermassen, J. B. Parys, and J.-P. Mauger, Biol. Cell **96**, 3 (2004).
[3] S. Zhang, A. Mizutani, C. Hisatsune, T. Higo, H. Bannai, T. Nakayama, M. Hattori, and M. Mikoshiba, J. Biol. Chem. **278**, 4048 (2003).
[4] M. Yamamoto-Hino, A. Miyawaki, A. Segawa, E. Adachi, S. Yamashina, T. Fujimotok, T. Sugiyama, T. Furuichi, M. Hasegawa, and K. Mikoshiba, J. Cell Biol. **141**, 135 (1998).
[5] O. H. Petersen and A. V. Tepikin, Annu. Rev. Physiol. **70**, 273 (2008).
[6] M. G. Lee, X. Xu, W. Zeng, J. Diaz, R. J. H. Wojcikiewicz, T. H. Kuo, F. Wuytack, L. Racymaekers, and S. Muallem, J. Biol. Chem. **272**, 15765 (1997).
[7] E. Hernandez, M. F. Leite, M. T. Guerra, E. A. Kruglov, O. Bruna-Romero, M. A. Rodrigues, D. A. Gomes, F. J. Giordano, J. A. Dranoff, and M. H. Nathanson, J. Biol. Chem. **282**, 10057 (2007).
[8] K. Kiselyov, X. Wang, D. M. Shin, W. Zang, and S. Muallem, Cell Calcium **40**, 451 (2006).
[9] T. Satoh, C. A. Ross, A. Villa, S. Supattapone, T. Pozzan, S. H. Snyder, and J. Meldolesi, J. Cell Biol. **111**, 615 (1990).
[10] O. Dellis, S. G. Dedos, S. C. Tovey, T. Ur-Rahman, S. J. Dubel, and C. W. Taylor, Science **313**, 229 (2006).
[11] P. Pinton, T. Pozzan, and R. Rizzuto, EMBO J. **17**, 5298 (1998).
[12] J. V. Gerasimenko, M. Sherwood, A. V. Tepikin, O. H. Petersen, and O. V. Gerasimenko, J. Cell. Sci. **119**, 226 (2006).
[13] W. Echevarría, M. F. Leite, M. T. Guerra, W. R. Zipfel, and M. H. Nathanson, Nat. Cell Biol. **5**, 440 (2003).
[14] E. Vermassen, K. Van Acker, W. G. Annaert, B. Himpens, G. Callewaert, L. Missiaen, H. De Smedt, and J. B. Parys, J. Cell. Sci. **116**, 1269 (2003).
[15] R. A. Fissore, F. J. Longo, E. Anderson, J. B. Parys, and T. Ducibella, Biol. Reprod. **60**, 49 (1999).
[16] K. J. Seymour-Laurent and M. E. Barish, J. Neurosci. **15**, 2592 (1995).
[17] A. H. Sharp, P. S. McPherson, T. M. Dawson, C. Aoki, K. P. Campbell, and S. H. Synder, J. Neurosci. **13**, 3051 (1993).

[18]N. Callamaras, X.-P. Sun, I. Ivorra, and I. Parker, J. Physiol. (London) **511**, 395 (1998).
[19]J. K. Foskett, C. White, K. H. Cheung, and D. O. Mak, Physiol. Rev. **87**, 593 (2007).
[20]K. Mikoshiba, J. Neurochem. **102**, 1426 (2007).
[21]P. Delmas, N. Wanaverbecq, F. C. Abogadie, M. Mistry, and D. A. Brown, Neuron **34**, 209 (2002).
[22]C. Sala, V. Piëch, N. R. Wilson, M. Passafaro, G. Liu, and M. Sheng, Neuron **31**, 115 (2001).
[23]I. Isshiki, J. Ando, K. Yamamoto, T. Fujita, Y. Ying, and R. G. W. Anderson, J. Cell. Sci. **115**, 475 (2002).
[24]J. Ledoux, M. S. Taylor, A. D. Bonev, R. M. Hannah, V. Solodushko, B. Shui, Y. Tallini, M. I. Kotikoff, and M. T. Nelson, Proc. Natl. Acad. Sci. U.S.A. **105**, 9627 (2008).
[25]A. K. Weaver, M. L. Olsen, M. B. McFerrin, and H. Sontheimer, J. Biol. Chem. **282**, 31558 (2007).
[26]S. C. Tovey, S. G. Dedos, E. J. Taylor, J. E. Church, and C. W. Taylor, J. Cell Biol. **183**, 297 (2008).
[27]A. Miyakawa-Naito, P. Uhlén, M. Lal, O. Aizman, K. Mikoshiba, H. Brismar, S. Zelenin, and A. Aperia, J. Biol. Chem. **278**, 50355 (2003).
[28]C. Wei, X. Wang, M. Chen, K. Ouyang, L. S. Song, and H. Cheng, Nature (London) **457**, 901 (2009).
[29]P. B. Simpson, S. Mehorta, G. D. Lange, and J. T. Russell, J. Biol. Chem. **272**, 22654 (1997).
[30]N. Callamaras and I. Parker, J. Gen. Physiol. **113**, 199 (1999).
[31]A. A. Khan, J. P. Steiner, M. G. Klein, M. F. Schneider, and S. H. Snyder, Science **257**, 815 (1992).
[32]B. S. Wilson, J. R. Pfeiffer, A. J. Smith, J. M. Oliver, J. A. Oberdorf, and R. J. H. Wojcikiewicz, Mol. Biol. Cell **9**, 1465 (1998).
[33]M. Chalmers, M. J. Schell, and P. Thorn, Biochem. J. **394**, 57 (2006).
[34]C. Soeller, D. Crossmam, R. Gilbert, and M. B. Cannell, Proc. Natl. Acad. Sci. U.S.A. **104**, 14958 (2007).
[35]C. Soeller, I. D. Jayasingle, P. Li, A. V. Holden, and M. B. Cannell, Exp. Physiol. **94**, 496 (2009).
[36]D.-O. D. Mak and J. K. Foskett, J. Gen. Physiol. **109**, 571 (1997).
[37]L. Ionescu, K. H. Cheung, H. Vais, D. O. Mak, C. White, and J. K. Foskett, J. Physiol. (London) **573**, 645 (2006).
[38]I. Parker, J. Choi, and Y. Yao, Cell Calcium **20**, 105 (1996).
[39]M. D. Bootman and M. J. Berridge, Cell **83**, 675 (1995).
[40]I. Parker and Y. Yao, Proc. R. Soc. London, Ser. B **246**, 269 (1991).
[41]X.-P. Sun, N. Callamaras, J. S. Marchant, and I. Parker, J. Physiol. (London) **509**, 67 (1998).
[42]D. Thomas, P. Lipp, M. J. Berridge, M. D. Bootman, J. Biol. Chem. **273**, 27130 (1998).
[43]M. G. Klein and M. F. Schneider, Prog. Biophys. Mol. Biol. **92**, 308 (2006).
[44]S. Guatimosim, K. Dilly, L. F. Santana, M. Saleet Jafri, E. A. Sobie, and W. J. Lederer, J. Mol. Cell. Cardiol. **34**, 941 (2002).
[45]H. J. Rose, S. Dargan, J. Shuai, and I. Parker, Biophys. J. **91**, 4024 (2006).
[46]J. Shuai, H. J. Rose, and I. Parker, Biophys. J. **91**, 4033 (2006).
[47]N. Callamaras, J. S. Marchant, X.-P. Sun, and I. Parker, J. Physiol. (London) **509**, 81 (1998).
[48]J. S. Marchant, N. Callamaras, and I. Parker, EMBO J. **18**, 5285 (1999).
[49]M. D. Bootman, E. Niggli, M. J. Berridge, and P. Lipp, J. Physiol. (London) **499**, 307 (1997).
[50]S. C. Tovey, P. De Smet, P. Lipp, D. Thomas, K. W. Young, L. Missiaen, H. De Smedt, J. B. Parys, M. J. Berridge, J. Thuring, A. Holmes, and M. D. Bootman, J. Cell Biol. **114**, 3979 (2001).
[51]M. D. Bootman, M. J. Berridge, and P. Lipp, Cell **91**, 367 (1997).
[52]J. S. Marchant and I. Parker, EMBO J. **20**, 65 (2001).
[53]D. Thomas, P. Lipp, S. C. Tovey, M. J. Berridge, W. Li, R. Y. Tsien, and M. D. Bootman, Curr. Biol. **10**, 1 (2000).
[54]J. S. Marchant, V. Ramos, and I. Parker, Am. J. Physiol. **282**, C1374 (2002).
[55]M. D. Bootman, P. Lipp, and M. J. Berridge, J. Cell. Sci. **114**, 2213 (2001).
[56]J. Shuai, J. E. Pearson, J. K. Foskett, D.-O. D. Mak, and I. Parker, Biophys. J. **93**, 1151 (2007).
[57]A. Demuro and I. Parker, Cell Calcium **43**, 367 (2008).
[58]C. W. Taylor, P. C. A. Da Fonseca, and E. P. Morris, Trends Biochem. Sci. **29**, 210 (2004).
[59]M. J. Boulware and J. S. Marchant, J. Physiol. (London) **586**, 2873 (2008).
[60]E. Katayama, H. Funahashi, T. Michikawa, T. Shiraishi, T. Ikemoto, M. Iino, K. Hirosawa, and K. Mikoshiba, EMBO J. **15**, 4844 (1996).
[61]C. C. Yin, L. M. Blayney, and F. A. Lai, J. Mol. Biol. **349**, 538 (2005).
[62]J. R. Groff and G. D. Smith, Biophys. J. **95**, 135 (2008).
[63]D. Bray and T. Duke, Annu. Rev. Biophys. Biomol. Struct. **33**, 53 (2004).
[64]S. Swillens, G. Dupont, L. Combettes, and P. Champeil, Proc. Natl. Acad. Sci. U.S.A. **96**, 13750 (1999).
[65]H. DeRemigio and J. R. Groff, Mathematical Medicine and Biology **25**, 65 (2008).
[66]T. Ur-Rahman, A. Skupin, M. Falcke, and C. W. Taylor, Nature (London) **458**, 655 (2009).
[67]M. Kalamvoki and B. Roizman, J. Virol. **81**, 6316 (2007).
[68]R. G. Kessel, Int. Rev. Cytol. **133**, 43 (1992).
[69]O. Stendahl, K.-H. Krause, J. Krischer, P. Jerström, J.-M. Theler, R. A. Clark, J.-L. Carpentier, and D. P. Lew, Science **265**, 1439 (1994).
[70]S. A. Stricker, Semin Cell Dev. Biol. **17**, 303 (2006).
[71]F. Mitsuyama and T. Sawai, Int. J. Dev. Biol. **45**, 861 (2001).
[72]J. G. Goetz, H. Genty, P. St-Pierre, T. Dang, B. Joshi, R. Sauvé, W. Vogl, and I. R. Nabi, J. Cell. Sci. **120**, 3553 (2007).
[73]V. C. Cordes, S. Reidenbach, and W. W. Franke, Cell Tissue Res. **284**, 177 (1996).
[74]K. Subramanian and T. Meyer, Cell **89**, 963 (1997).
[75]J. Andrade, H. Zhao, B. Titus, S. T. Pearce, and M. Barroso, Mol. Biol. Cell **15**, 481 (2004).
[76]S. A. Stricker and T. L. Smythe, Development **130**, 2867 (2003).
[77]A. A. Pieper, D. J. Brat, E. O'Hearn, D. K. Krug, A. I. Kaplin, K. Takahashi, J. H. Greenberg, D. Ginty, M. E. Molliver, and S. H. Snyder, Neuroscience **102**, 433 (2001).
[78]J. Liou, L. M. Kim, W. D. Heo, J. T. Jones, J. W. Myers, J. E. Ferrell, Jr., and T. Meyer, Curr. Biol. **15**, 1235 (2005).
[79]J. Roos, P. J. DiGregorio, A. V. Yeromin, K. Ohlsen, M. Lioudyno, S. Zhang, O. Safrina, J. A. Kozak, S. L. Wagner, M. D. Cahalan, G. Velicelebi, and K. A. Stauderman, J. Cell Biol. **169**, 435 (2005).
[80]M. Ferreri-Jacobia, D. O. Mak, and J. K. Foskett, J. Biol. Chem. **280**, 3824 (2005).
[81]K. Fukatsu, H. Bannai, S. Zhang, H. Nakamura, T. Inoue, and K. Mikoshiba, J. Biol. Chem. **279**, 48976 (2004).
[82]C. Cruttwell, J. Bernard, M. Hilly, V. Nicolas, R. E. A. Tunwell, and J.-P. Mauger, Biol. Cell **97**, 699 (2005).
[83]D. Boehning and S. K. Joseph, J. Biol. Chem. **275**, 21492 (2000).
[84]M. Iwai, Y. Tateishi, M. Hattori, A. Mizutani, T. Nakamura, A. Futatsugi, T. Inoue, T. Furuichi, T. Michikawa, and K. Mikoshiba, J. Biol. Chem. **280**, 10305 (2005).
[85]Y. Tojyo, T. Morita, A. Nezu, and A. Tanimura, J. Pharmacol. Sci. **107**, 138 (2008).
[86]Y. Tateishi, M. Hattori, T. Nakayama, M. Iwai, H. Bannai, T. Nakamura, T. Michikawa, T. Inoue, and K. Mikoshiba, J. Biol. Chem. **280**, 6816 (2005).
[87]K. Machaca, Dev. Biol. **275**, 170 (2004).
[88]M. Hattori, A. Z. Suzuki, T. Higo, H. Miyaucji, T. Michikawa, T. Nakamoura, T. Inoue, and K. Mikoshiba, J. Biol. Chem. **279**, 11967 (2004).
[89]K. Hamada, T. Miyata, K. Mayanagi, J. Hirota, and K. Mikoshiba, J. Biol. Chem. **277**, 21115 (2002).
[90]B. Alarcon, M. Swamy, H. M. van Santen, and W. W. A. Schamel, EMBO Rep. **7**, 490 (2006).
[91]Y. Zhang, S. E. McKay, B. Bewley, and L. K. Kaczmarek, J. Biol. Chem. **283**, 10632 (2008).
[92]H. Misonou, D. P. Mohapatra, E. W. Park, V. Leung, D. Zhen, K. Misonou, A. E. Anderson, and J. S. Trimmer, Nat. Neurosci. **7**, 711 (2004).
[93]M. L. Molina, F. N. Barrera, A. M. Fernández, J. A. Poveda, M. L. Renart, J. A. Encinar, G. Riquelme, and J. M. González-Ros, J. Biol. Chem. **281**, 18837 (2006).
[94]A. Penna, A. Demuro, A. V. Yeromin, S. L. Zhang, O. Safrina, I. Parker, and M. D. Cahalan, Nature (London) **456**, 116 (2008).
[95]K. D. Mossman, G. Campi, J. T. Groves, and M. L. Dustin, Science **310**, 1191 (2005).
[96]T. Yokosuka, K. Sakata-Sogawa, W. Kobayashi, M. Hiroshima, A. Hashimoto-Tane, M. Tokunga, M. L. Dustin, and T. Saito, Nature Immunology **6**, 1253 (2005).
[97]C. Zhang and S.-H. Kim, Pac. Symp. Biocomput., 353 (2000).
[98]M. Gopalakrishnan, K. Forsten-Williams, M. A. Nugent, U. C. Täuber, Biophys. J. **89**, 3686 (2005).
[99]D. Bray, M. D. Levin, and C. J. Morton-Firth, Nature (London) **393**, 85 (1998).
[100]S. Valitutti, S. Müller, M. Cella, E. Padovan, and A. Lanzavecchia, Nature (London) **375**, 148 (1995).

[101] S. Means, A. J. Smith, J. Shepherd, J. Shadid, J. Fowler, R. J. H. Wojcikiewicz, T. Mazel, G. D. Smith, and B. S. Wilson, Biophys. J. **91**, 537 (2006).
[102] L. Missiaen, H. De Smedt, G. Droogmans, and R. Casteels, Nature (London) **357**, 599 (1992).
[103] T. Higo, M. Hattori, T. Nakamura, T. Natsume, T. Michikawa, and K. Mikosiba, Cell **120**, 85 (2005).
[104] C. W. Taylor, A. A. Genazzani, and S. A. Morris, Cell Calcium **26**, 237 (1999).
[105] K. Takei, G. A. Mignery, E. Mugnaini, T. C. Südhof, and P. De Camilli, Neuron **12**, 327 (1994).
[106] J. W. Shuai and P. Jung, Proc. Natl. Acad. Sci. U.S.A. **100**, 506 (2003).
[107] J. W. Shuai and P. Jung, Phys. Rev. Lett. **88**, 068102 (2002).
[108] E. Hong-Geller and R. A. Cerione, J. Cell Biol. **148**, 481 (2000).